

Heterogeneity-Aware Dataset Scheduling for Efficient Audio Large Language Model Training

Yanru Wu¹ Jianning Wang² Chongxin Gan³ Yang Li^{1*}

¹Shenzhen International Graduate School, Tsinghua University

²Independent Researcher

³The Hong Kong Polytechnic University

Abstract

Training general-purpose Audio Large Language Models (ALLMs) across diverse datasets is essential for holistic audio understanding, yet it faces significant challenges due to dataset heterogeneity, which often leads to conflicting gradients and slow convergence. Despite its impact, how to explicitly manage this heterogeneity during training remains underexplored, with current practices relying primarily on uniform mixture. In this work, we analyze multi-dataset AudioQA training from a convergence perspective and propose Grouped Sequential Training (GST). GST strategically organizes datasets into affinity-aware groups and introduces them via a progressive scheduling protocol, effectively balancing the stability of parallel training with the efficiency of sequential optimization. To ensure scalability, we develop gradient-based affinity metrics that capture inter-dataset relationships without the prohibitive cost of empirical transferability estimation. Extensive evaluations on 14 AudioQA datasets spanning speech, music, and environmental sounds demonstrate that GST achieves 30–40% faster convergence than standard parallel training while maintaining or even surpassing the performance of mix-all training. Our results provide both theoretical insights and a practical, model-agnostic framework for efficient large-scale ALLM optimization.

1 Introduction

Large language models (LLMs) have recently been extended beyond text to incorporate audio perception, enabling progress in tasks such as classification, captioning, and question answering (Kong et al., 2024; Hurst et al., 2024). Among these, AudioQA (Gong et al., 2023) has attracted increasing attention as a unified data format for training Audio LLMs (ALLMs), consolidating diverse audio tasks into a single framework and supporting

broad application scenarios from assistive technology to human–computer interaction. While recent efforts have integrated pretrained audio encoders into LLMs to build general-purpose AudioQA models (Chu et al., 2024; Tang et al., 2024), scaling across datasets with disparate domains, annotation styles, and difficulty levels introduces significant yet often overlooked training inefficiencies.

Multi-task learning (Zhang and Yang, 2021) provides a natural theoretical lens for generalization across diverse datasets, where in practice each dataset is often treated as an instantiation of a task. Extensive explorations have been conducted in traditional machine learning (Standley et al., 2020; Liu et al., 2019), encompassing investigations of curriculum learning (Soviany et al., 2022), task sampling (Sharma et al., 2017), and various training paradigms (Elich et al., 2024). However, these approaches typically rely on task-specific assumptions, architectural modifications, or auxiliary training mechanisms, limiting their applicability to general ALLMs.¹ Consequently, most existing ALLM training pipelines resort to naive strategies such as uniform dataset mixing, and fail to account for substantial data heterogeneity. Although such mixing ensures task coverage, it often induces suboptimal training dynamics characterized by redundant updates and slow convergence. These inefficiencies are further exacerbated in ALLMs by the inherent complexities of long audio sequences, cross-modal alignment, and the sheer scale of the models.

Recent advances in taskonomy and transferability estimation (Zamir et al., 2018; Wang et al., 2025) have established that dataset-level relationships can be successfully quantified. Yet despite this progress, a systematic understanding of how dataset-level heterogeneity governs the training of ALLMs remains elusive. Current analyses are largely restricted to post-hoc evaluations, leaving

*Corresponding Author

¹See Sec. 2.2 for further discussion.

a gap in understanding how these heterogeneous traits directly impact real-time training dynamics, and more importantly, how they can inform the design of training strategies. Building on this intuition, this work addresses a central question: How can these dataset properties be explicitly leveraged to schedule efficient multi-dataset training for ALLMs, thereby accelerating convergence without architectural overheads?

To address this, we investigate multi-dataset training for ALLMs through the lens of convergence analysis. We begin by theoretically analyzing the convergence behaviors of different training regimes, focusing on how gradient variance and dataset heterogeneity affect training dynamics. Our analysis reveals the relative advantages of parallel versus sequential training under differing heterogeneity degrees, which then motivates our proposal of Grouped Sequential Training (GST). As a paradigm that interpolates between parallel and sequential optimization, GST organizes datasets into groups with reduced intra-group heterogeneity. By executing sequential updates at the group level, this strategy yields provably tighter convergence bounds in realistic multi-dataset settings. For practical implementation, we cluster datasets using metrics that capture optimization-level disparities, such as gradient-based distance and empirical transferability. To further scale the framework to large-scale ALLMs, we introduce an efficient progressive training procedure that approximates grouped sequential optimization while minimizing computational overhead and mitigating catastrophic forgetting. Importantly, our approach is model-agnostic and requires no architectural modifications. Extensive evaluations across 14 AudioQA datasets demonstrate that our method significantly accelerates convergence compared to naive multi-task baselines, while simultaneously maintaining or enhancing performance across diverse domains. Our contributions can be summarized as follows:

- **Theoretical Framework:** We establish a convergence analysis for ALLMs that rigorously characterizes the impact of gradient variance and dataset heterogeneity.
- **Paradigm Shift:** We propose Grouped Sequential Training (GST), which interpolates between parallel and sequential optimization and moves dataset affinity estimation from post-hoc analysis into training loop design.
- **Scalable Implementation:** We introduce a progressive training procedure that approximates the optimal grouping strategy, enabling efficient large-scale training without architectural changes.
- **Benchmark & Insights:** We consolidate 14 datasets into a unified AudioQA format, providing systematic insights and actionable strategies for heterogeneous multi-dataset training.

2 Related Works

2.1 Audio Large Language Model

ALLMs have transformed audio-related tasks by demonstrating remarkable zero-shot performance and classification, understanding, and reasoning capabilities. Existing approaches typically adopt either an encoder-only or an encoder-decoder architecture (Saeed et al., 2021). The encoder-only paradigm employs a dual-tower framework where the text and audio encoders process paired text-audio data. Following the training objective of Contrastive Language-Image Pre-training (CLIP) (Radford et al., 2021), such models are trained to learn a joint embedding space by drawing the embeddings of paired data closer while pushing apart those of unpaired data.

In parallel, driven by the success of vision-language models, various encoder-decoder ALLMs have been proposed to leverage the large language model for audio comprehension. Prior works such as SALMONN (Tang et al., 2024), Pengi (Deshmukh et al., 2023), Qwen-Audio (Chu et al., 2023, 2024), and the Audio Flamingo series (Kong et al., 2024; Ghosh et al., 2025; Goel et al., 2025) have achieved state-of-the-art performances across a wide range of audio tasks. Those methods integrate an audio encoder with a decoder-only language model in a cascade manner. Unlike encoder-only methods that solely rely on contrastive training objectives, encoder-decoder ALLMs are trained with generative objectives, such as masked reconstruction or next-token prediction. This paradigm enables the model to capture richer semantic audio information, facilitating more flexible reasoning and instruction-following abilities.

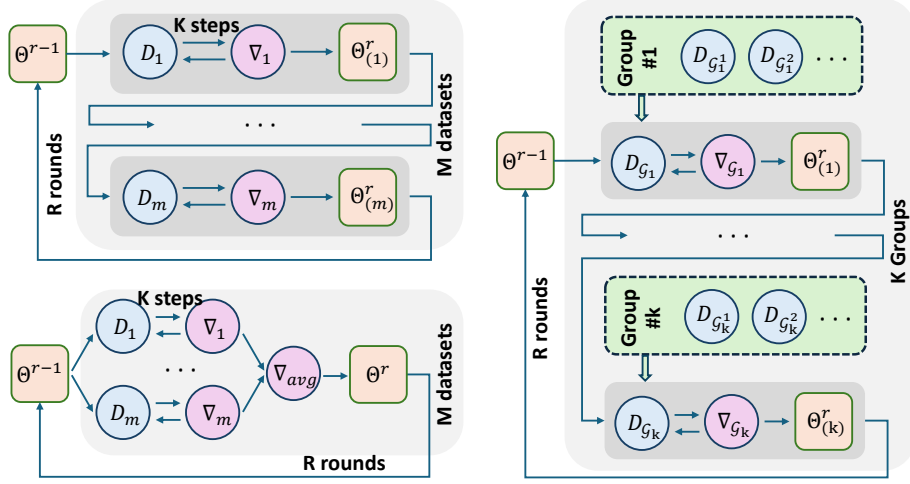


Figure 1: **Illustration of sequential (left-up), parallel (left-down), and grouped sequential training (right).**

2.2 Training Strategies for Multi-Dataset Learning

Training models on multiple datasets is a fundamental challenge across multi-task (Zhang and Yang, 2021), continual (Kirkpatrick et al., 2017), and federated learning (Li et al., 2020). In the context of LLMs, research has increasingly shifted from purely architectural innovations (Houlsby et al., 2019; Shazeer et al., 2017) to data-centric optimization strategies. While substantial progress has been made in data selection and sampling weighting (Xie et al., 2023; Chen et al., 2023; Li et al., 2024) to curate optimal training mixtures, the role of learning scheduling remains underexplored.

Existing paradigms generally fall into two categories: parallel and sequential training (Fig. 1). Parallel training jointly optimizes all datasets via uniform mixing or weighted sampling (Raffel et al., 2020). While stable, it often suffers from gradient interference (Yu et al., 2020), where conflicting optimization directions from diverse domains lead to suboptimal convergence. In contrast, sequential training introduces datasets chronologically (Bengio et al., 2009). While this can prioritize high-quality data to bootstrap representations, it risks catastrophic forgetting of earlier tasks and often lacks a principled basis for determining the optimal sequence. Most theoretical analyses (Koloskova et al., 2020; Li and Lyu, 2023), often established within the context of federated optimization, are confined to idealized formulations, focusing on the two extremes: fully parallel or strictly sequential regimes. Strategies that interpolate between these extremes, such as data-driven grouping (Standley et al., 2020) or stage-wise scheduling (Zamir et al.,

2018), often lack systematic, convergence-oriented analyses tailored for dataset-level ALLM training. Furthermore, their post-hoc design and task dependency hinder their integration into the dynamic training loops of large-scale models.

3 Problem Setup

3.1 Formulation

Modern ALLMs unify diverse audio understanding tasks through a shared language interface, enabling natural language reasoning over acoustic signals (Latif et al., 2023). Consider the multi-dataset training problem for AudioQA. Let $\mathcal{D} = \{D_m\}_{m=1}^M$ denote a collection of M datasets, where each dataset $D_m = \{(a_i, x_i, y_i)\}_{i=1}^{N_m}$ consists of audio inputs a_i and their corresponding textual question-answer pairs (x_i, y_i) .

Given a model f parameterized by Θ , our objective is to minimize the aggregate loss across all tasks:

$$\min_{\Theta} \left\{ F(\Theta) := \frac{1}{M} \sum_{m=1}^M F_m(\Theta) \right\}, \quad (1)$$

where $F_m(\theta)$ denotes the task-specific loss on D_m , measured by cross-entropy in our ALLM training. Following standard ALLM architectures (Tang et al., 2024), we initialize f from a pretrained LLM backbone (e.g., a LLaMA-style decoder) and extend it to the audio modality with audio feature extractors and learnable adapters (e.g., LoRA layers), while the backbone weights maintain frozen.

3.2 Characterizing Dataset Heterogeneity

Despite sharing a common input-output format, AudioQA datasets exhibit pronounced heterogeneity

due to acoustic characteristics, annotation styles, and task complexities. To rigorously quantify this, we adopt the gradient decomposition framework from federated optimization (Li and Lyu, 2023), characterizing heterogeneity through gradient inconsistency across datasets:

$$\frac{1}{M} \sum_{m=1}^M \|\nabla F_m(\Theta) - \nabla F(\Theta)\|^2 \leq \beta^2 \|\nabla F(\Theta)\|^2 + \zeta^2, \quad (2)$$

where the constants β and ζ capture the degree of dataset-level divergence. Intuitively, larger values of β^2 and ζ^2 indicate stronger disagreement among gradients derived from different datasets, a phenomenon known to impede convergence in both sequential and parallel optimization regimes. In the context of ALLMs, such gradient inconsistency is not merely an artifact of distribution shifts but reflects intrinsic semantic disparities. For example, datasets emphasizing temporal localization may induce gradients that prioritize fine-grained acoustic cues, whereas captioning datasets favor global semantic representations. These differences persist even when datasets are projected onto a unified language output space, necessitating a more sophisticated training strategy than naive mixing.

4 Methodology

4.1 Sequential and Parallel Training under Dataset Heterogeneity

To analyze the impact of dataset heterogeneity, we first establish a theoretical foundation, measuring convergence by the minimum expected gradient norm across R training rounds:

$$\mathcal{C}(R) := \min_{0 \leq r \leq R} \mathbb{E}[\|\nabla F(\Theta^{(r)})\|^2], \quad (3)$$

where the convergence rate is characterized by the decay of $\mathcal{C}(R)$ with respect to R . We then adapt the theoretical findings from federated learning (Li and Lyu, 2023) to the multi-dataset setting by treating each dataset as a distinct ‘‘client’’, simplifying the complex distributed dynamics into two primary factors - stochastic gradient variance and dataset heterogeneity. Specifically, we have the following assumptions and results:

AS1 (Smoothness): Each dataset-specific objective F_m is L -smooth.

AS2 (Bounded Variance): The gradient computed on each dataset has a variance bounded by σ^2 .

AS3 (Bounded Heterogeneity): Dataset-level heterogeneity is bounded by constants β and ζ as defined in Eqn. (2).

Lemma 1 (Par. and Seq. Training Convergence)

Under Assumptions AS1–AS3, the convergence rates for parallel and sequential training over M datasets satisfy:

$$\mathcal{C}_{par} = \mathcal{O}\left(\frac{A\sigma}{R^{\frac{1}{2}}} + \frac{B\sigma^{\frac{2}{3}} + C\zeta^{\frac{2}{3}}}{R^{\frac{2}{3}}} + \frac{D(1 + \beta^2)}{R}\right), \quad (4)$$

$$\mathcal{C}_{seq} = \mathcal{O}\left(\frac{A\sigma}{R^{\frac{1}{2}}} + \frac{B\sigma^{\frac{2}{3}} + C\zeta^{\frac{2}{3}}}{M^{\frac{1}{3}}R^{\frac{2}{3}}} + \frac{D(1 + \frac{\beta^2}{M})}{R}\right), \quad (5)$$

where A, B, C, D are positive constants depending on the smoothness L and optimization hyperparameters.

Comparing the bounds in Lemma 1 reveals a fundamental trade-off. Parallel training benefits from joint sampling, which stabilizes optimization and reduces the effective σ^2 . However, it is fully exposed to the global heterogeneity terms β^2 and $\zeta^{2/3}$. In contrast, sequential training suppresses these heterogeneity effects by factors of $1/M$ and $1/M^{1/3}$, effectively ‘‘decoupling’’ the interference between divergent datasets at the cost of losing joint variance reduction. Consequently, while parallel mixing is robust for mild heterogeneity, the sequential regime becomes theoretically superior as dataset divergence increases - as is common in complex ALLM tasks. This observation suggests that neither extreme is globally optimal, motivating a strategy that balances variance reduction with heterogeneity suppression.

4.2 Grouped Sequential Training (GST)

AudioQA datasets often exhibit structured heterogeneity. For instance, datasets involving music perception share closer optimization trajectories than those requiring speech comprehension. To capture this structure and achieve the ‘‘best of both worlds’’ discussed in Sec. 4.1, we propose to partition the M datasets into K affinity-based groups $\{\mathcal{G}_k\}_{k=1}^K$ and conduct Grouped Sequential Training (GST), a hybrid paradigm that leverages local variance reduction while maintaining global heterogeneity suppression (Fig. 1). For each group, the group-level objective is defined as:

$$F^{(k)}(\Theta) := \frac{1}{M_k} \sum_{m \in \mathcal{G}_k} F_m(\Theta), \quad (6)$$

where M_k is the number of datasets in \mathcal{G}_k and $F^{(k)}$ inherits L -smoothness from its constituent datasets. The global gradient variance can thus be decomposed as follows:

Proposition 1 (Heterogeneity Decomposition)

For any partition $\{\mathcal{G}_k\}_{k=1}^K$, the global gradient variance can be decomposed into intra-group and inter-group components:

$$\underbrace{\frac{1}{M} \sum_{m=1}^M \|\nabla F_m - \nabla F\|^2}_{\text{Global Variance}} \quad (7)$$

$$= \underbrace{\frac{1}{M} \sum_{k=1}^K \sum_{m \in \mathcal{G}_k} \|\nabla F_m - \nabla F^{(k)}\|^2}_{\text{Intra-group Heterogeneity}} \quad (8)$$

$$+ \underbrace{\frac{1}{M} \sum_{k=1}^K M_k \|\nabla F^{(k)} - \nabla F\|^2}_{\text{Inter-group Heterogeneity}}. \quad (9)$$

Following this decomposition, we characterize heterogeneity bound at two levels: intra-group (β_k, ζ_k) and inter-group (β_g, ζ_g) . Analogous to Eqn. (2), they satisfy:

$$\begin{aligned} \frac{1}{M_k} \sum_{m \in \mathcal{G}_k} \|\nabla F_m(\Theta) - \nabla F^{(k)}(\Theta)\|^2 \\ \leq \beta_k^2 \|\nabla F^{(k)}(\Theta)\|^2 + \zeta_k^2, \end{aligned} \quad (10)$$

$$\begin{aligned} \frac{1}{K} \sum_{k=1}^K \|\nabla F^{(k)}(\Theta) - \nabla F(\Theta)\|^2 \\ \leq \beta_g^2 \|\nabla F(\Theta)\|^2 + \zeta_g^2. \end{aligned} \quad (11)$$

We establish the relationship between group-wise and global heterogeneity from Prop. 1:

Lemma 2 (Heterogeneity Bound) For a grouping strategy that clusters datasets with high affinities, the intra-group and inter-group heterogeneity constants satisfy:

$$\text{(Intra-group): } \beta_k^2 \leq \beta^2, \quad \zeta_k^2 \leq \zeta^2, \quad (12)$$

$$\begin{aligned} \text{(Inter-group): } \beta_g^2 &\leq \frac{M\beta^2}{KM_{min}} - \Gamma_{\mathcal{G}}, \\ \zeta_g^2 &\leq \frac{M\zeta^2}{KM_{min}} - \Delta_{\mathcal{G}}, \end{aligned} \quad (13)$$

where M_{min} is the smallest group size, and $\Gamma_{\mathcal{G}}, \Delta_{\mathcal{G}} \geq 0$ are the residual terms representing the heterogeneity absorbed within groups via affinity-based alignment.

The proof is given in Appendix A.1.2.

Based on Lemma 2, GST satisfies the three fundamental optimization assumptions: (i) $F^{(k)}$ inherits L -smoothness; (ii) the stochastic gradient variance within groups is bounded by $\sigma_k^2 < \sigma^2$ guaranteed by the bound of intra-group heterogeneity (β_k, ζ_k) ; ² and (iii) inter-group heterogeneity is bounded by (β_g, ζ_g) . We then apply the convergence results at the group level and have:

Theorem 1 (Convergence of GST) Under Assumptions AS1–AS3, the convergence rate of Grouped Sequential Training satisfies:

$$C_{gst} = \mathcal{O} \left(\frac{A\sigma_g}{R^{\frac{1}{2}}} + \frac{B\sigma_g^{\frac{2}{3}} + C\zeta_g^{\frac{2}{3}}}{K^{\frac{1}{3}}R^{\frac{2}{3}}} + \frac{D(1 + \frac{\beta_g^2}{K})}{R} \right). \quad (14)$$

Theorem 1 identifies GST as a superior middle ground. By optimizing over K groups rather than M datasets, GST suppresses the impact of inter-group heterogeneity by factors of $1/K^{1/3}$ and $1/K$. Crucially, as shown in Lemma 2, proper grouping ensures that the inter-group divergence (β_g, ζ_g) remains a controlled fraction of the global heterogeneity. Meanwhile, the joint training within each group retains the variance reduction benefit ($\sigma_k < \sigma$) typical of parallel mixing. Consequently, the GST bound is strictly tighter than that of fully parallel training in Eqn. (4), which is hindered by large global heterogeneity, and fully sequential training in Eqn. (5), which suffers from unmitigated stochastic noise.

4.3 Affinity-Aware Grouped Training

To implement the GST strategy, we require an affinity-aware mechanism to partition datasets. Following our convergence analysis, our primary objective is to cluster datasets with high optimization affinities to minimize the intra-group divergence (β_k, ζ_k) . This ensures that the parallel mixing within each group remains stable, while the residual inter-group heterogeneity is effectively compressed through the sequential stages of GST.

Gradient-Based Affinity. We quantify affinity via the pairwise distance between dataset-level gradients. Based directly on the notion of heterogeneity in Eqn. (2), we define the dataset distance as:

$$\text{Dist}(T_m, T_n) = \|\nabla F_m(\Theta) - \nabla F_n(\Theta)\|^2, \quad (15)$$

²Refer to Appendix A.1.3 for the proof.

where $\sum_{m,n=1}^M \|\nabla F_m(\Theta) - \nabla F_n(\Theta)\|^2 = M \cdot \sum_{m=1}^M \|\nabla F_m(\Theta) - \nabla F(\Theta)\|^2$.

A smaller distance signifies a higher affinity, indicating that the datasets share consistent optimization trajectories. In practice, we estimate $Dist(D_m, D_n)$ through a controlled probing procedure: starting from a common initialization, we finetune the model on each dataset for a fixed number of steps and accumulate the gradients. We then apply spectral clustering on the resulting distance matrix to form the task groups $\{\mathcal{G}_k\}$.

Alternative: Empirical Transferability. We also consider an empirical transferability based criterion (Zamir et al., 2018) as a complementary baseline.³ This measure evaluates affinity by observing cross-dataset performance gains:

$$Trf(D_m \rightarrow D_n) = \frac{F_n(\Theta_m) - F_n(\Theta_n)}{F_n(\Theta_n)}. \quad (16)$$

Here Θ_m, Θ_n denote the model parameters after training on D_m and D_n respectively. While intuitive, this metric is computationally expensive (requiring M^2 testing pairs) and less directly coupled with the optimization dynamics in Theorem 1. We thus primarily use it for comparative analysis.

Training Implementation: From Sequential to Progressive. While Theorem 1 assumes strict sequential transitions, repeatedly cycling through groups after short update intervals can present significant practical hurdles to large-scale ALLM training, entailing catastrophic forgetting and prohibitive data loading overhead. To bridge this gap, we adopt in practice a Progressive Grouped Training schedule: we begin with group \mathcal{G}_1 and incrementally expand the training pool to $\bigcup_{j=1}^{k+1} \mathcal{G}_j$ at each subsequent stage. This progressive expansion serves as an efficient approximation of GST; it mitigates initial gradient conflicts through sequential introduction while maintaining the stability and I/O throughput of joint mixing. Consequently, this hybrid regime balances the variance reduction of parallel training with the heterogeneity suppression of the sequential regime.

5 Experiments

5.1 Experimental Setup

We empirically evaluate our proposed data-level training strategy to verify if the theoretical advan-

³A discussion of the affinity metrics and dataset relationships is included in Appendix A.4.

tages of GST translate into superior performance and convergence in ALLM training.

Model Architecture. We select SALMONN-13B (Tang et al., 2024) as our experimental platform. While newer models have emerged, SALMONN remains a highly representative and open-source foundation for ALLMs, featuring a standard architecture that combines a Whisper encoder with a Vicuna-13B backbone. Its well-documented training pipeline makes it an ideal testbed for isolating the effects of dataset scheduling from architectural innovations. We strictly follow the official configuration to ensure all gains stem solely from GST strategy. The performance is then evaluated by token-level prediction accuracy.

AudioQA Dataset Formulation. We evaluate our method on 14 diverse datasets covering speech, music, and environmental sounds. Following (Gong et al., 2023), all tasks are unified into an AudioQA format. This collection serves as a benchmark for structured heterogeneity in general audio perception, with significant variations in annotation style and domain-specific knowledge. Dataset descriptions are detailed in Appendix A.2.

Training Strategies. We evaluate several canonical dataset scheduling strategies. To ensure a rigorous controlled experiment, all methods share identical model architectures, optimization settings, and training budgets, differing only in their dataset organization:⁴ **Parallel Training:** Jointly optimizes by uniformly sampling data from all 14 datasets at each iteration; **Sequential Training:** Optimizes datasets one at a time in a fixed order, representing a zero-mixing extreme; **Independent Training:** Finetunes a separate model for each dataset, serving as an empirical upper bound for single-task performance; **GST (Proposed):** Our affinity-aware strategy. To explore the granularity and criteria of grouping, we evaluate three variants, i.e. **GST-T2**, Taskonomy-based grouping ($K = 2$) using empirical transferability (Eqn. 16), and **GST-G2 / G3**, Gradient-based grouping ($K = 2 / K = 3$) using gradient distance (Eqn. 15). Unless otherwise noted, we employ the Progressive implementation for stability.

5.2 Main Results

We evaluate training strategies under two distinct settings to comprehensively assess their impact on

⁴Training details are provided in Appendix A.3.

	D1	D2	D3	D4	D5	D6	D7	D8	D9	D10	D11	D12	D13	D14	Avg	W.Avg	$\mathcal{T.E.}$
SALMONN	50.7	39.4	52.4	88.9	90.8	55.1	35.4	70.0	66.3	61.4	9.9	40.5	39.8	53.8	53.9	54.1	N/A
Individual	60.1	96.7	47.5	98.0	91.3	96.5	44.6	92.8	62.9	90.8	77.5	64.9	83.6	63.1	76.4	77.0	~7d
Sequential	42.7	35.2	47.0	61.6	92.4	28.4	33.7	56.0	56.9	63.5	14.6	45.6	41.0	61.1	48.6	54.3	~7d
Mix All	56.1	94.9	50.6	97.6	87.9	95.0	47.4	89.5	67.1	87.6	72.8	55.4	76.5	62.2	74.3	74.2	~4d
GST-T2	58.8	96.2	52.8	97.9	89.0	95.9	48.4	90.6	66.3	90.9	73.3	60.6	72.9	62.2	75.4	74.5	~2d
GST-G3	56.7	96.0	52.4	98.0	90.1	95.8	48.6	88.8	66.2	88.2	73.7	57.3	79.6	62.1	75.2	75.0	~2d
GST-G2	55.4	95.1	51.9	97.6	88.3	95.5	47.4	91.0	67.4	87.2	70.8	57.0	79.9	61.6	74.7	74.6	~2d
Mix All	52.1	93.1	46.3	93.9	89.5	92.1	41.4	91.4	60.5	81.2	67.7	45.8	54.1	52.9	68.7	63.9	~0.5d
GST-T2	50.9	94.7	46.9	96.0	87.1	93.2	41.1	91.6	61.4	82.9	69.4	43.8	53.8	53.8	69.0	64.7	~0.5d
GST-G3	48.2	95.2	46.5	96.4	88.9	93.7	41.2	91.6	58.9	81.5	69.0	52.5	51.1	52.1	69.1	63.4	~1d
GST-G2	50.4	93.6	46.1	96.1	89.3	93.4	40.1	92.0	60.6	82.0	69.5	44.1	53.6	51.0	68.7	63.5	~0.5d

Table 1: **Token-Level Accuracy(%) Comparison in Full-Data Training (Up) and Low-Resource Finetuning (Down).** $D_1 \dots D_{14}$ correspond to: AudioCaps, ChimeHome, Clotho, CochScene, IEMOCAP, Jamendo, MACS, MusicNet, MusicQA, OpenAQA, PromptSpeech, SoundDescs, TextrolSpeech, and WavCaps, respectively.

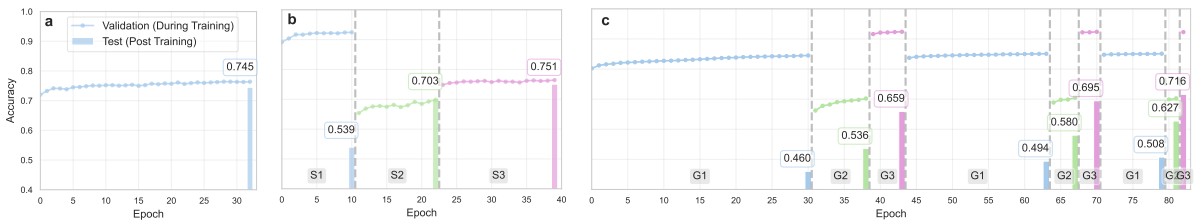


Figure 2: **Comparison of training dynamics and convergence across different scheduling protocols.** (a), (b), and (c) represent Mix-all, GST (Progressive), and GST (Strict Sequential), respectively. The curves denote the validation accuracy across training epochs, while the bars indicate the average test accuracy across all datasets at the end of each stage.

Schedule	Avg	W.Avg	Avg	W.Avg
Progressive*	75.2	75.0	74.7	74.6
Reverse Progressive	72.1	72.1	72.9	72.6
Strict Cycle Sequential	70.7	64.0	60.3	68.2

Table 2: **Accuracy(%) Comparison of Ordering Strategies in Full-Data Training.** We evaluate different curriculums using the grouping criteria of GST-G3 (left) and GST-G2 (right). “*” denotes our method.

optimization:

Full-Data Training: Utilizing all available data and training from scratch, this setting emulates the large-scale joint training phase typical in building foundation models.

Low-Resource Finetuning: Capping each dataset at $N = 250$ samples and initializing from SALMONN checkpoints, this setting emulates supervised finetuning of models with scarce data.

Tab. 1 summarizes the performance across 14 AudioQA datasets. We report the raw testing accuracy for each task, along with the cumulative time elapsed ($\mathcal{T.E.}$) and two aggregate metrics: the un-

weighted average accuracy (Avg), and the sample-size weighted average accuracy (W.Avg).

5.2.1 Performance on Full-Data Training

As illustrated in Tab. 1, the performance of GST strategies in full-data training is characterized by: **Superior Performance.** Our proposed GST variants consistently outperform Parallel Training (Mix-all). Specifically, GST-T2 achieves the highest unweighted average, while GST-G3 leads in the weighted average. Notably, all variants significantly exceed the Original SALMONN baseline and closely approach the Independent Training reference (the empirical upper bound), underscoring the validity of our experimental comparison.

Robustness Against Forgetting. Compared to Sequential Training, which suffers from a drastic drop in accuracy due to catastrophic forgetting, our GST implementation maintains a high performance ceiling, confirming that the progressive introduction of groups serves as an effective buffer.

Enhanced Optimization Efficiency. A key highlight of our results is the significant reduction in

training time. While the parallel baseline requires approximately 4 days to reach convergence, GST variants complete the process within 2–3 days. This 30–40% speedup in large-scale training empirically validates the tighter convergence bounds derived in Theorem 1.

5.2.2 Stability in Low-Resource Scenarios

In the low-resource regime, the primary challenge shifts from managing massive heterogeneity to ensuring sample efficiency. We omit the Sequential baseline here as it leads to severe forgetting with sparse data, yielding non-informative results. Findings for the remaining strategies are as follows:

Performance Stability. In the low-resource regime, GST variants achieve comparable performance to the Parallel baseline. This result notably demonstrates that the group-wise sequential nature of GST does not compromise the model’s adaptation capability even under extreme data sparsity.

Diminishing Acceleration Returns. Unlike the full-data regime, the training acceleration effect is less pronounced here, with marginal reductions in wall-clock time. This phenomenon can be attributed to a trade-off between heterogeneity suppression and early-stage overfitting: when training on a small initial group \mathcal{G}_1 , the model may rapidly overfit to these sparse samples before the data pool expands. Consequently, the potential time gains from reduced gradient variance are partially offset by the optimization overhead required to stabilize learning on such limited data.

5.3 Discussion

5.3.1 Convergence Behaviors

To further investigate how GST features in optimization dynamics, we plot in Fig. 2 the training of three representative strategies: Mix-all, GST-G3 (Strict Sequential), and GST-G3 (Progressive). As depicted in the curves, Strict Sequential training exhibits a “volatile” pattern; while performance peaks at the end of each stage, it suffers drastic drops upon returning to previous data groups (e.g., from Stage 3 back to Stage 1), characterizing classic catastrophic forgetting. This instability forces the model to undergo significantly more training cycles to reach a stable state. In contrast, Progressive GST maintains a steady and monotonic improvement in test accuracy, proving the effectiveness of our progressive implementation. Compared with Mix-All, Progressive GST also reaches a stable performance plateau slightly earlier (approx. epoch

25 vs. epoch 27). More importantly, the per-epoch training time for Mix-all is substantially longer than that of GST. We attribute this to the high gradient heterogeneity in Mix-all, which forces the optimizer to reconcile conflicting update directions within every batch, leading to higher computational overhead and slower stable descent.

5.3.2 Impact of Group Ordering: The Stability-First Curriculum

To examine how the temporal sequence of dataset groups influences the optimization trajectory, we compare three scheduling strategies: Strict Cycle Sequential, Progressive, and Reverse Progressive (see Tab. 2). Our analysis reveals that the effectiveness of GST is highly sensitive to the initial training phase and the data retention mechanism. The superiority of the positive Progressive order over the Reverse variant underscores a “stability-first” curriculum effect. When high-variance or outlier tasks are introduced prematurely (as in the Reverse order), the model encounters a “noisy” initialization phase that is both computationally expensive and optimizationally destructive. A complex initial group not only requires excessive epochs to reach marginal convergence but also forces the model into suboptimal regions of the loss landscape. Furthermore, the poor performance of Strict Cycle Sequential highlights the danger of abrupt distribution shifts introduced by the original sequential strategy. These results confirm that an affinity-aware initialization and optimization stability are essential for navigating the complex heterogeneity of multi-dataset ALLM training.

6 Conclusion

In this paper, we introduced Grouped Sequential Training (GST), a principled optimization framework designed to mitigate the challenges of gradient heterogeneity in multi-dataset ALLM training. By strategically grouping datasets based on affinity measures and introducing them via a progressive scheduling protocol, GST effectively balances inter-dataset interference and optimization efficiency. Theoretically, we derived tighter convergence bounds for GST, demonstrating that reducing intra-group gradient variance directly accelerates stable descent. Empirically, evaluations across 14 diverse AudioQA datasets show that GST variants not only outperform parallel and sequential training baselines but also achieve a 30–40% reduction in training time. Our findings underscore the im-

portance of affinity-aware scheduling in large-scale joint training and provide a scalable, interpretable pathway for developing robust ALLMs.

7 Limitations

While the proposed GST framework demonstrates significant acceleration and stability in ALLM training, we acknowledge several limitations that open avenues for future research.

Diversity of Backbones and Frameworks. Our current evaluation is primarily conducted using the SALMONN framework with a Vicuna-13B backbone. Although these are representative of state-of-the-art audio-language models, the scalability of GST to even larger models (e.g., 70B parameters) or different architectural paradigms (e.g., MoE-based audio LLMs) remains to be extensively verified. Future work will investigate whether the gradient affinity patterns observed here persist across diverse model scales and initialization states.

Bottleneck Analyses in Mix-all Training Efficiency. We observed that the Mix-all baseline exhibits slower per-epoch training speeds compared to partitioned strategies. Our profiling indicates this is not merely due to data loading overhead, but stems from gradient variance explosion in the early stages of training. When heterogeneous datasets are shuffled into a single stream, the frequent directional shifts in gradients (∇F_m) lead to unstable optimizer states and more rejected updates in the loss landscape. GST mitigates this by grouping consistent signals, but a more rigorous theoretical quantification of this "mixing penalty" is still needed.

Refinement of the "Stability-First" Ordering. Our Stability-First ordering strategy (beginning with high-affinity, low-variance groups) is based on the heuristic that establishing a robust representation early on prevents computational waste and optimizational destruction. However, a purely optimal ordering might require a more dynamic approach. The current static ordering, while effective, does not account for the temporal evolution of dataset relationships—as the model learns, two datasets that were initially conflicting might become synergistic. Exploring a dynamic, feedback-driven ordering mechanism is a promising direction.

References

Yoshua Bengio, Jérôme Louradour, Ronan Collobert, and Jason Weston. 2009. Curriculum learning. In

Proceedings of the 26th annual international conference on machine learning, pages 41–48.

Carlos Busso, Murtaza Bulut, Chi-Chun Lee, Abe Kazemzadeh, Emily Mower, Samuel Kim, Jeanette N Chang, Sungbok Lee, and Shrikanth S Narayanan. 2008. Iemocap: Interactive emotional dyadic motion capture database. *Language resources and evaluation*, 42(4):335–359.

Mayee Chen, Nicholas Roberts, Kush Bhatia, Jue Wang, Ce Zhang, Frederic Sala, and Christopher Ré. 2023. Skill-it! a data-driven skills framework for understanding and training language models. *Advances in Neural Information Processing Systems*, 36:36000–36040.

Yunfei Chu, Jin Xu, Qian Yang, Haojie Wei, Xipin Wei, Zhifang Guo, Yichong Leng, Yuanjun Lv, Jinzheng He, Junyang Lin, and 1 others. 2024. Qwen2-audio technical report. *arXiv preprint arXiv:2407.10759*.

Yunfei Chu, Jin Xu, Xiaohuan Zhou, Qian Yang, Shiliang Zhang, Zhijie Yan, Chang Zhou, and Jingren Zhou. 2023. Qwen-audio: Advancing universal audio understanding via unified large-scale audio-language models. *arXiv preprint arXiv:2311.07919*.

Soham Deshmukh, Benjamin Elizalde, Rita Singh, and Huaming Wang. 2023. Pengi: An audio language model for audio tasks. *Advances in Neural Information Processing Systems*, 36:18090–18108.

Konstantinos Drossos, Samuel Lipping, and Tuomas Virtanen. 2020. Clotho: An audio captioning dataset. In *ICASSP 2020-2020 IEEE International Conference on Acoustics, Speech and Signal Processing (ICASSP)*, pages 736–740. IEEE.

Cathrin Elich, Lukas Kirchdorfer, Jan M Köhler, and Lukas Schott. 2024. Examining common paradigms in multi-task learning. In *DAGM German Conference on Pattern Recognition*, pages 131–147. Springer.

Peter Foster, Siddharth Sigtia, Sacha Krstulovic, Jon Barker, and Mark D Plumbley. 2015. Chime-home: A dataset for sound source recognition in a domestic environment. In *2015 IEEE Workshop on Applications of Signal Processing to Audio and Acoustics (WASPAA)*, pages 1–5. IEEE.

Jort F Gemmeke, Daniel PW Ellis, Dylan Freedman, Aren Jansen, Wade Lawrence, R Channing Moore, Manoj Plakal, and Marvin Ritter. 2017. Audio set: An ontology and human-labeled dataset for audio events. In *2017 IEEE international conference on acoustics, speech and signal processing (ICASSP)*, pages 776–780. IEEE.

Sreyan Ghosh, Zhifeng Kong, Sonal Kumar, S Sakshi, Jaehyeon Kim, Wei Ping, Rafael Valle, Dinesh Manocha, and Bryan Catanzaro. 2025. Audio flamingo 2: An audio-language model with long-audio understanding and expert reasoning abilities. In *Forty-second International Conference on Machine Learning*.

- Arushi Goel, Sreyan Ghosh, Jaehyeon Kim, Sonal Kumar, Zhifeng Kong, Sang-gil Lee, Chao-Han Huck Yang, Ramani Duraiswami, Dinesh Manocha, Rafael Valle, and Bryan Catanzaro. 2025. Audio flamingo 3: Advancing audio intelligence with fully open large audio language models. *arXiv preprint arXiv:2507.08128*.
- Yuan Gong, Hongyin Luo, Alexander H Liu, Leonid Karlinsky, and James Glass. 2023. Listen, think, and understand. *arXiv preprint arXiv:2305.10790*.
- Zhifang Guo, Yichong Leng, Yihan Wu, Sheng Zhao, and Xu Tan. 2023. Promptts: Controllable text-to-speech with text descriptions. In *ICASSP 2023-2023 IEEE International Conference on Acoustics, Speech and Signal Processing (ICASSP)*, pages 1–5. IEEE.
- Neil Houlsby, Andrei Giurgiu, Stanislaw Jastrzebski, Brando Brunskill, Erik Cassou, and 1 others. 2019. Parameter-efficient transfer learning for nlp. In *International Conference on Machine Learning (ICML)*, pages 2790–2799.
- Aaron Hurst, Adam Lerer, Adam P Goucher, Adam Perelman, Aditya Ramesh, Aidan Clark, AJ Ostrow, Akila Welihinda, Alan Hayes, Alec Radford, and 1 others. 2024. Gpt-4o system card. *arXiv preprint arXiv:2410.21276*.
- Il-Young Jeong and Jeongsoo Park. 2022. Cochlsene: Acquisition of acoustic scene data using crowdsourcing. In *2022 Asia-Pacific Signal and Information Processing Association Annual Summit and Conference (APSIPA ASC)*, pages 17–21. IEEE.
- Shengpeng Ji, Jialong Zuo, Minghui Fang, Ziyue Jiang, Feiyang Chen, Xinyu Duan, Baoxing Huai, and Zhou Zhao. 2024. Textrolspeech: A text style control speech corpus with codec language text-to-speech models. In *ICASSP 2024-2024 IEEE International Conference on Acoustics, Speech and Signal Processing (ICASSP)*, pages 10301–10305. IEEE.
- Chris Dongjoo Kim, Byeongchang Kim, Hyunmin Lee, and Gunhee Kim. 2019. Audiocaps: Generating captions for audios in the wild. In *Proceedings of the 2019 Conference of the North American Chapter of the Association for Computational Linguistics: Human Language Technologies, Volume 1 (Long and Short Papers)*, pages 119–132.
- James Kirkpatrick, Razvan Pascanu, Neil Rabinowitz, Joel Veness, Guillaume Desjardins, and 1 others. 2017. Overcoming catastrophic forgetting in neural networks. *Proceedings of the National Academy of Sciences (PNAS)*, 114(13):3521–3526.
- A Sophia Koepke, Andreea-Maria Oncescu, João F Henriques, Zeynep Akata, and Samuel Albanie. 2022. Audio retrieval with natural language queries: A benchmark study. *IEEE Transactions on Multimedia*, 25:2675–2685.
- Junyoung Koh, Soo Yong Kim, Yongwon Choi, and Gyu Hyeon Choi. 2025. Jamendo-qa: A large-scale music question answering dataset. *arXiv preprint arXiv:2509.15662*.
- Anastasia Koloskova, Nicolas Loizou, Sadra Boreiri, Martin Jaggi, and Sebastian Stich. 2020. A unified theory of decentralized sgd with changing topology and local updates. In *International conference on machine learning*, pages 5381–5393. PMLR.
- Zhifeng Kong, Arushi Goel, Rohan Badlani, Wei Ping, Rafael Valle, and Bryan Catanzaro. 2024. Audio flamingo: A novel audio language model with few-shot learning and dialogue abilities. In *International Conference on Machine Learning*, pages 25125–25148. PMLR.
- Siddique Latif, Moazzam Shoukat, Fahad Shamshad, Muhammad Usama, Yi Ren, Heriberto Cuayáhuil, Wenwu Wang, Xulong Zhang, Roberto Togneri, Erik Cambria, and 1 others. 2023. Sparks of large audio models: A survey and outlook. *arXiv preprint arXiv:2308.12792*.
- Jeffrey Li, Alex Fang, Georgios Smyrnis, Maor Ivgi, Matt Jordan, Samir Yitzhak Gadre, Hritik Bansal, Etash Guha, Sedrick Scott Keh, Kushal Arora, and 1 others. 2024. Datacomp-lm: In search of the next generation of training sets for language models. *Advances in Neural Information Processing Systems*, 37:14200–14282.
- Tian Li, Anit Kumar Sahu, Ameet Talwalkar, and Virginia Smith. 2020. Federated learning: Challenges, methods, and future directions. *IEEE signal processing magazine*, 37(3):50–60.
- Yipeng Li and Xinchun Lyu. 2023. Convergence analysis of sequential federated learning on heterogeneous data. *Advances in Neural Information Processing Systems*, 36:56700–56755.
- Shansong Liu, Atin Sakkeer Hussain, Chenshuo Sun, and Ying Shan. 2024. Music understanding llama: Advancing text-to-music generation with question answering and captioning. In *ICASSP 2024-2024 IEEE International Conference on Acoustics, Speech and Signal Processing (ICASSP)*, pages 286–290. IEEE.
- Shikun Liu, Edward Johns, and Andrew J Davison. 2019. End-to-end multi-task learning with attention. In *Proceedings of the IEEE/CVF conference on computer vision and pattern recognition*, pages 1871–1880.
- Irene Martín-Morató and Annamaria Mesaros. 2021. What is the ground truth? reliability of multi-annotator data for audio tagging. In *2021 29th European Signal Processing Conference (EUSIPCO)*, pages 76–80. IEEE.
- Xinhao Mei, Chutong Meng, Haohe Liu, Qiuqiang Kong, Tom Ko, Chengqi Zhao, Mark D Plumbley, Yuexian Zou, and Wenwu Wang. 2024. Wavcaps: A chatgpt-assisted weakly-labelled audio captioning dataset for audio-language multimodal research. *IEEE/ACM Transactions on Audio, Speech, and Language Processing*, 32:3339–3354.

- Alec Radford, Jong Wook Kim, Chris Hallacy, Aditya Ramesh, Gabriel Goh, Sandhini Agarwal, Girish Sastry, Amanda Askell, Pamela Mishkin, Jack Clark, and 1 others. 2021. Learning transferable visual models from natural language supervision. In *International conference on machine learning*, pages 8748–8763. PmlR.
- Colin Raffel, Noam Shazeer, Adam Roberts, Katherine Lee, Sharan Narang, Michael Matena, Yanqi Zhou, and Peter J Liu. 2020. Exploring the limits of transfer learning with a unified text-to-text transformer. *Journal of Machine Learning Research*, 21(140):1–67.
- Aaqib Saeed, David Grangier, and Neil Zeghidour. 2021. Contrastive learning of general-purpose audio representations. In *ICASSP 2021-2021 IEEE International Conference on Acoustics, Speech and Signal Processing (ICASSP)*, pages 3875–3879. IEEE.
- Sahil Sharma, Ashutosh Jha, Parikshit Hegde, and Balaraman Ravindran. 2017. Learning to multi-task by active sampling. *arXiv preprint arXiv:1702.06053*.
- Noam Shazeer, Azalia Mirhoseini, Krzysztof Maziarz, Andy Davis, Quoc Le, Geoffrey Hinton, and Jeff Dean. 2017. Outrageously large neural networks: The sparsely-gated mixture-of-experts layer. *arXiv preprint arXiv:1701.06538*.
- Petru Soviany, Radu Tudor Ionescu, Paolo Rota, and Nicu Sebe. 2022. Curriculum learning: A survey. *International Journal of Computer Vision*, 130(6):1526–1565.
- Trevor Standley, Amir Zamir, Dawn Chen, Leonidas Guibas, Jitendra Malik, and Silvio Savarese. 2020. Which tasks should be learned together in multi-task learning? In *International conference on machine learning*, pages 9120–9132. PMLR.
- Changli Tang, Wenyi Yu, Guangzhi Sun, Xianzhao Chen, Tian Tan, Wei Li, Lu Lu, Zejun MA, and Chao Zhang. 2024. SALMONN: Towards generic hearing abilities for large language models. In *The Twelfth International Conference on Learning Representations*.
- John Thickstun, Zaid Harchaoui, and Sham Kakade. 2016. Learning features of music from scratch. *arXiv preprint arXiv:1611.09827*.
- Haohua Wang, Jingge Wang, Zijie Zhao, Yang Tan, Yanru Wu, Hanbing Liu, Jingyun Yang, Enming Zhang, Xiangyu Chen, Zhengze Rong, and 1 others. 2025. Understanding knowledge transferability for transfer learning: A survey. *arXiv preprint arXiv:2507.03175*.
- Sang Michael Xie, Hieu Pham, Xuanyi Dong, Nan Du, Hanxiao Liu, Yifeng Lu, Percy S Liang, Quoc V Le, Tengyu Ma, and Adams Wei Yu. 2023. Doremi: Optimizing data mixtures speeds up language model pretraining. *Advances in Neural Information Processing Systems*, 36:69798–69818.
- Tianhe Yu, Saurabh Kumar, Abhishek Gupta, Sergey Levine, Karol Hausman, and Chelsea Finn. 2020. Gradient surgery for multi-task learning. In *Advances in Neural Information Processing Systems (NeurIPS)*, volume 33, pages 5824–5836.
- Amir R Zamir, Alexander Sax, William Shen, Leonidas J Guibas, Jitendra Malik, and Silvio Savarese. 2018. Taskonomy: Disentangling task transfer learning. In *Proceedings of the IEEE conference on computer vision and pattern recognition*, pages 3712–3722.
- Yu Zhang and Qiang Yang. 2021. A survey on multi-task learning. *IEEE transactions on knowledge and data engineering*, 34(12):5586–5609.

A Appendix

A.1 Theoretical Proof

A.1.1 Proof of Prop. 1 (Heterogeneity Decomposition)

For any dataset m belonging to group \mathcal{G}_k , we decompose the deviation from the global mean by inserting the group mean $\nabla F^{(k)}$:

$$\|\nabla F_m - \nabla F\|^2 \quad (17)$$

$$= \|(\nabla F_m - \nabla F^{(k)}) + (\nabla F^{(k)} - \nabla F)\|^2 \quad (18)$$

Expanding the squared norm:

$$\|\nabla F_m - \nabla F\|^2 \quad (19)$$

$$= \|\nabla F_m - \nabla F^{(k)}\|^2 + \|\nabla F^{(k)} - \nabla F\|^2 \quad (20)$$

$$+ 2\langle \nabla F_m - \nabla F^{(k)}, \nabla F^{(k)} - \nabla F \rangle \quad (21)$$

Summing over all datasets $m \in \{1, \dots, M\}$:

$$\sum_{M=1}^m \|\nabla F_m - \nabla F\|^2 \quad (22)$$

$$= \sum_{k=1}^K \sum_{m \in \mathcal{G}_k} \|\nabla F_m - \nabla F\|^2 \quad (23)$$

$$= \sum_{k=1}^K \sum_{m \in \mathcal{G}_k} \|\nabla F_m - \nabla F^{(k)}\|^2 \quad (24)$$

$$+ \sum_{k=1}^K \sum_{m \in \mathcal{G}_k} \|\nabla F^{(k)} - \nabla F\|^2 + \text{Cross Terms} \quad (25)$$

$$= \sum_{k=1}^K \sum_{m \in \mathcal{G}_k} \|\nabla F_m - \nabla F^{(k)}\|^2 \quad (26)$$

$$+ M_k \sum_{k=1}^K \|\nabla F^{(k)} - \nabla F\|^2 + \text{Cross Terms}, \quad (27)$$

where Cross Terms = 0, due to:

$$2 \sum_{m \in \mathcal{G}_k} \langle \nabla F_m - \nabla F^{(k)}, \nabla F^{(k)} - \nabla F \rangle \quad (28)$$

$$= 2 \underbrace{\left\langle \sum_{m \in \mathcal{G}_k} (\nabla F_m - \nabla F^{(k)}), \nabla F^{(k)} - \nabla F \right\rangle}_0 = 0. \quad (29)$$

Therefore, we have

$$\frac{1}{M} \sum_{m=1}^M \|\nabla F_m - \nabla F\|^2 \quad (30)$$

$$= \frac{1}{M} \sum_{k=1}^K \sum_{m \in \mathcal{G}_k} \|\nabla F_m - \nabla F^{(k)}\|^2 \quad (31)$$

$$+ \frac{1}{M} \sum_{k=1}^K M_k \|\nabla F^{(k)} - \nabla F\|^2. \quad (32)$$

A.1.2 Proof of Lemma 2 (Heterogeneity Bound)

For intra-group heterogeneity, we have:

$$\begin{aligned} & \frac{1}{K} \sum_{k=1}^K \|\nabla F^{(k)}(\Theta) - \nabla F(\Theta)\|^2 \\ & \leq \frac{M}{KM_{min}} \cdot \frac{1}{M} \sum_{k=1}^K M_k \|\nabla F^{(k)}(\Theta) - \nabla F(\Theta)\|^2 \\ & \leq \frac{M\beta^2}{KM_{min}} \|\nabla F(\Theta)\|^2 + \frac{M\zeta^2}{KM_{min}} \\ & \quad - \frac{1}{KM_{min}} \sum_{k=1}^K \sum_{m \in \mathcal{G}_k} \|\nabla F_m(\Theta) - \nabla F^{(k)}(\Theta)\|^2. \end{aligned} \quad (33)$$

Comparing Eqn. (33) with the form of bound in Eqn. (11), we have $\zeta_g^2 < \frac{M\zeta^2}{KM_{min}} - \Gamma_G$ and $\beta_g^2 < \frac{M\beta^2}{KM_{min}} - \Delta_G$, with M_{min} denoting the smallest group size and $\Gamma_G, \Delta_G \geq 0$ are the residual terms representing the heterogeneity absorbed within groups via affinity-based alignment.

A.1.3 Proof of Stochastic Gradient Variance

Noting the stochastic gradient on dataset m as $g_m(\Theta)$ and stochastic gradient in \mathcal{G}_k as $g^{(k)}(\Theta)$, for the intra-group stochastic gradient variance, we have:

$$\|g^{(k)} - \nabla F^{(k)}\|^2 \quad (34)$$

$$= \left\| \frac{1}{M_k} \sum_{m \in \mathcal{G}_k} (g_m - \nabla F_m) \right\|^2 \quad (35)$$

$$+ \frac{1}{M_k} \sum_{m \in \mathcal{G}_k} (\nabla F_m - \nabla F^{(k)})^2 \quad (36)$$

$$\leq \left\| \frac{1}{M_k} \sum_{m \in \mathcal{G}_k} (g_m - \nabla F_m) \right\|^2 \quad (37)$$

$$+ \left\| \frac{1}{M_k} \sum_{m \in \mathcal{G}_k} (\nabla F_m - \nabla F^{(k)}) \right\|^2, \quad (38)$$

with

$$\mathbb{E} \left\| \frac{1}{M_k} \sum_{m \in \mathcal{G}_k} (g_m - \nabla F_m) \right\|^2 \quad (39)$$

$$\leq \frac{1}{M_k^2} \sum_{m \in \mathcal{G}_k} \mathbb{E} \|g_m - \nabla F_m\|^2 \leq \frac{\sigma^2}{M_k}, \quad (40)$$

$$\left\| \frac{1}{M_k} \sum_{m \in \mathcal{G}_k} (\nabla F_m - \nabla F^{(k)}) \right\|^2 \quad (41)$$

$$\leq \frac{1}{M_k} \sum_{m \in \mathcal{G}_k} \|\nabla F_m - \nabla F^{(k)}\|^2 \quad (42)$$

$$\leq \beta_k^2 \|\nabla F^{(k)}\|^2 + \zeta_k^2. \quad (43)$$

Hence, we have

$$\mathbb{E} \left[\left\| g^{(k)} - \nabla F^{(k)} \right\|^2 \right] \quad (44)$$

$$\leq \frac{\sigma^2}{M_k} + \beta_k^2 \|\nabla F^{(k)}\|^2 + \zeta_k^2 = \sigma_k^2. \quad (45)$$

Here σ_k is given by $\frac{\sigma^2}{M_k}$ and intra-group heterogeneity (β_k, ζ_k) , and $\sigma_k < \sigma$ can be ensured with bounded intra-group heterogeneity.

A.2 Dataset Description

To evaluate the proposed GST framework across diverse acoustic scenarios, we curate a comprehensive benchmark consisting of 14 datasets covering ambient sounds, speech, and music. These datasets are categorized into three primary types of tasks: Audio Captioning (CAP), Audio Question Answering (AQA), and Audio Classification (CLS). For classification tasks, we follow a standard ‘‘Classification to QA’’ prompting strategy to ensure compatibility with LLM instruction-following. For classification tasks, we follow a standard ‘‘Classification to QA’’ prompting strategy to ensure compatibility with LLM instruction-following. Specifically, we list the datasets below:

- **Ambient & General Audio:** We include AudioCaps (Kim et al., 2019), Clotho_v2 (Drossos et al., 2020), WavCaps (Mei et al., 2024), and MACS (Martín-Morató and Mesaros, 2021) for general audio captioning. SoundDescs (Koepeke et al., 2022) provides fine-grained descriptions, while OpenQA (Gong et al., 2023) (derived from AudioSet (Gemmeke et al., 2017)) offers large-scale temporal audio reasoning.
- **Acoustic Scenes:** ChimeHome (Foster et al., 2015) and CochScene (Jeong and Park, 2022)

are used for scene recognition. To adapt these CLS datasets for ALLM training, we hard-code labels into natural language QA pairs (e.g., ‘‘Where is the audio recorded?’’ → ‘‘The audio is recorded in a car.’’).

- **Music Analysis:** MusicQA (Liu et al., 2024), MusicNet (Thickstun et al., 2016), and Jamendo (Koh et al., 2025) cover music captioning, ensemble recognition, and mood analysis.
- **Speech & Emotion:** IEMOCAP (Busso et al., 2008) is utilized for emotion recognition using SALMONN annotations. PromptSpeech (Guo et al., 2023) and TextrolSpeech (Ji et al., 2024) provide speech-to-captioning tasks focusing on speaker traits and style.

A.3 Details of Training Settings

Model Architecture & Configuration. We build our model based on the SALMONN framework. The architecture consists of a dual-encoder system: a Whisper-Large-v2 for speech feature extraction and a BEATs (iter3+) for audio semantic encoding. Both encoders are kept frozen during training to preserve their pre-trained acoustic representations. A window-level Q-Former is employed to aggregate audio features with a window size and stride of 0.33 seconds, compressing the sequence into a single query token per window. To efficiently adapt the large language model, we utilize Vicuna-13B-v1.1 as the backbone and integrate Parameter-Efficient Fine-Tuning (PEFT) via LoRA. The LoRA adapters are applied with a rank $r = 8$ and $\alpha = 32$, significantly reducing the number of trainable parameters while maintaining competitive performance.

Optimization Details. The model is optimized using the AdamW optimizer with a weight decay of 0.05 and $\beta_2 = 0.999$. We employ a learning rate schedule starting with a warmup of 3,000 steps, increasing from $1e-6$ to a peak of $3e-5$, followed by a cosine decay to a minimum of $1e-5$. The training is conducted over a maximum of 30 epochs, with an early stopping patience of 5 epochs based on validation loss to prevent overfitting.

Hardware & Distributed Training. Our training infrastructure and hyperparameter settings vary based on the data scale:

- **Full-resource Training:** Conducted on a cluster of $4 \times$ NVIDIA A100 (80GB) GPUs. We

Table 3: Statistical overview of the multi-dataset benchmark used in this study. D_1 to D_{14} cover a diverse range of audio domains and tasks.

Dataset	Task Type	Primary Domain	Train	Val	Test
AudioCaps	CAP	General Audio	30,741	3,804	3,804
ChimeHome	CLS \rightarrow QA	Household	4,378	879	880
Clotho_v2	CAP	General Audio	3,839	1,045	1,045
CochlScene	CLS \rightarrow QA	Urban Scenes	60,855	7,573	7,687
IEMOCAP	CLS \rightarrow QA	Speech Emotion	3,272	409	409
Jamendo	QA	Music	26,090	3,261	3,261
MACS	CAP	Ambient Sound	3,144	393	393
MusicNet	QA	Classical Music	264	33	33
MusicQA	QA	General Music	42,867*	70,011	5,040
OpenAQA	Temporal QA	Multi-domain	213,158	26,644	26,644
PromptSpeech	CAP	Speech Style	21,272	2,658	2,658
SoundDescs	CAP	Environmental	26,452	3,306	3,306
TextrolSpeech	CAP	Speech Style	188,717	23,589	23,589
WavCaps	CAP	Large-scale Web	321,420	40,177	40,178
Total	-	-	946,469	183,782	119,030

* For MusicQA, we use the pretrain (42,867) for training and finetune (70,011) sets for validation.

Table 4: Comparison of Dataset Relationship Metrics: Taskonomy-based vs. Gradient-based.

Property	Taskonomy-based Metric	Gradient-based Metric (GST)
Symmetry	Insymmetric	Inherently symmetric ($A_{i,j} = A_{j,i}$)
Computational Cost	Extremely low (Pre-computed)	High (Requires per-dataset backprop)
Size Sensitivity	Yes ; heavily biased by sample counts	No ; focuses on directional alignment
Stability	Static throughout the training process	Dynamic; evolves with the model state
Representativeness	Semantic and label-level relationships	Optimization and landscape-level essence

use a batch size of 4 per GPU with an accumulation step of 1, resulting in an effective global batch size of 16.

- **Low-resource Training:** For specific ablation studies, we use $2 \times$ NVIDIA A100 GPUs, with the batch size per GPU and other configurations kept consistent, effectively halving the global batch size to 8.

All experiments are implemented using the Singularity container platform for environment consistency. Automatic Mixed Precision (AMP) is enabled to accelerate training and reduce memory footprint.

To evaluate the model’s performance and convergence efficiency across the multi-dataset benchmark, we employ Token-level Accuracy as our primary metric. This metric is defined as the ratio of correctly predicted tokens to the total number of

target tokens in the sequence:

$$Acc_{token} = \frac{\sum \text{Correct Tokens}}{\sum \text{Total Tokens}} \quad (46)$$

Unlike sentence-level metrics which can be overly sensitive to minor variations in decoding, Token-level Accuracy provides a high-resolution view of the model’s optimization progress. It directly reflects the model’s ability to minimize the cross-entropy loss across heterogeneous datasets, making it an ideal proxy for analyzing the convergence behaviors of different training protocols such as Mix-all and GST.

A.4 Interpreting Dataset Relationships: Gradient vs. Taskonomy-Based Metrics

Comparison of Metric Characteristics. As shown in Fig. 3, both metrics capture certain aspects of dataset interdependencies. While showing some coarse consistency, it is notable that Taskonomy is sensitive to dataset scale. For instance,

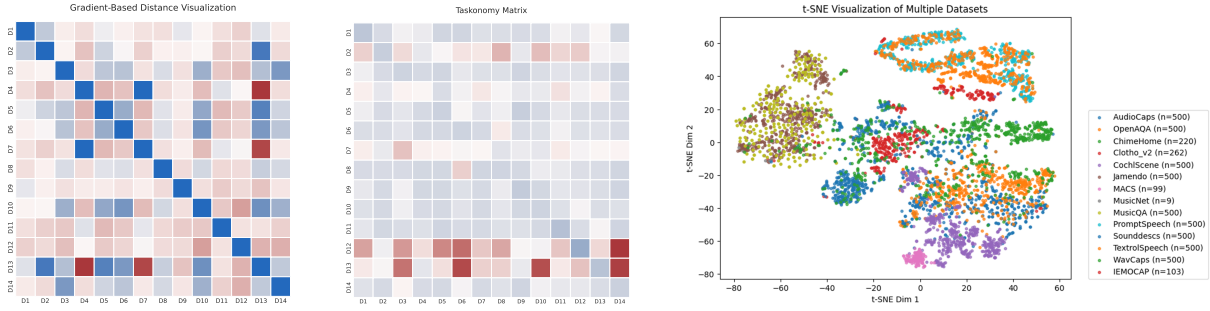


Figure 3: **Visualization of Dataset Relationship Measurements.** (a) Taskonomy-based Affinity Matrix and (b) Gradient-based Affinity Matrix, where blue indicates higher similarity (closer relationship) and red indicates lower similarity (further distance). (c) t-SNE Visualization of Acoustic Features, demonstrating distinct clustering based on audio domains (e.g., Music, Speech, Environmental).

large-scale datasets like WavCaps (321k) and OpenQA (213k) tend to negatively affect the learning of other datasets, creating "gravity wells" in the affinity matrix. They also differ significantly in their mathematical and computational properties, as shown in Tab. 4.

The Acoustic-Optimization Gap. To further investigate the "Audio" specificity, we performed a t-SNE visualization on the latent acoustic features extracted from the frozen encoders (Fig. 3).

- **Acoustic Clustering:** The t-SNE plot reveals clear, distinct clusters aligned with human-defined domains: Music (MusicQA, Jamendo), Speech (IEMOCAP, PromptSpeech), and Environmental sounds (ChimeHome, CochScene).
- **The Discrepancy:** Interestingly, neither our Taskonomy-based nor Gradient-based metrics strictly favor these acoustic domains. A music dataset may show higher gradient affinity with a speech-captioning dataset than with another music-tagging task.

This discrepancy indicates that the AudioQA relationship is influenced by factors far more complex than raw acoustic similarity. In a generative ALLM framework, the optimization direction ∇F_m is a joint product of **Acoustic spectral features** (the "what" is being heard), **Instruction complexity and label distribution** (the "how" it is being answered), and **Backbone alignment state** (the current mapping of audio to Vicuna tokens). While t-SNE captures the "acoustic appearance", our Gradient-based metric captures the "optimization essence".